Magneto-ionic propagation effects on incoherent scattered radar signals at small magnetic aspect angles

Berat Levent GEZER[1]

***Abstract*—Incoherent scatter radars are powerful tools to observe the dynamics of the upper atmosphere. We will describe an incoherent scatter radar operational model for linear polarized transmission and reception by two cross polarized linear antennas. The propagation medium is magneto-ionic. The code based on magneto-ionic model will describe how polarization changes with the scattering height and how this polarization change can be detected to remote sense the scattering medium. It willl also be shown how these polarization changes due to magneto-ionic effects distort the spectral shapes of the scattered signals.**

***Index Terms*—Magneto-ionic theory; incoherent scatter radar; covariance; aspect angle; Appleton-Hartree equation, ordinary and extraordinary modes.**

I. Introduction

Since it was constructed in 1961, Jicamarca Radio Obervatory (JRO) located in Lima, Peru, has been a premier tool for scientists, physcists, and engineers who want to study and understand the upper atmosphere. JRO is an incoherent scatter radar which has three 1.5 MW transmitters, 18,432 dipoles and a 85,000 m^2 antenna field. We can measure ionospheric electron and ion temperature, electron density, and plasma velocity information from Jicamarca incoherent scattered radar signals.

Since it was developed by J. P. Dougherty, and D. T. Farley in 1960 [1], incoherent scattering radar (ISR) theory for collisionless plasma has been revised a couple of times [2], [3]. The need to include the ion Coulomb collisions in the theory was first pointed out by D.T. Farley in 1964 [4] and a quantitative collisional model was first developed by R. Woodman as a part of his PhD thesis [5]. P. Sulzer and S. Gonzales showed that electron Coulomb collisions must also be included in the theory to account for the observed ISR spectra measured in Jicamarca at small magnetic aspect angles [6] for plasma drift measurements.

Their model was valid at the magnetic aspect angles greater than 0.1°. Within the magnetic aspect angle range from 0° to 0.1°, ISR spectrum sharpens substantially [7], and in this regime a 3-D extension of the model developed by *Kudeki* and *Milla* is needed *[7], [8]* . Forward modelling of small aspect angle ISR probing can be developed by using the *Kudeki* and *Milla* ISR model with magneto-ionic propagation model as explained here.

Department of Electrical and Computer Engineering, University of Illinois at Urbana-Champaign, Urbana, Illinois, USA

In this manuscript we focus on magneto-ionic propagation effects on the incoherent scattered radar signals. We model the co- and cross-polarized voltage spectra for different magnetic aspect angles which can be combined to form models of spectra measured by a finite width antenna beams. Section II presents this model. In Section III the results obtained from the model are presented and the paper is concluded with Section IV.

II. Magneto-ionic propagation model at small aspect angles

When a signal is transmitted through a magnetized plasma, it experiences changes in its polarization during its travel. The magneto-ionic propagation of a radiowave is analyzed using the coordinate system in Figure 1. The magnetic field $\vec{B}_o$ is on the yz-plane, the propagation vector $\vec{k}$ is parallel to the $\hat{z}$-direction. Unit vectors $\hat{\theta}$ and $\hat{\phi}$ are defined on the xy-plane and orthogonal to $\hat{k}$ [9].

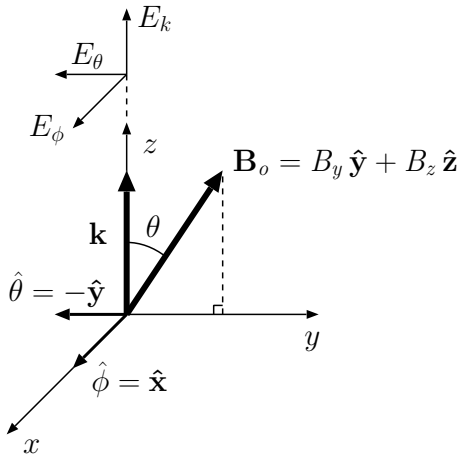

Figure 1. Coordinate system to display the propagation of a wave in a magnetized plasma [9].

The geometry of the problem given in Figure 1 can take many forms over the antenna field of JRO. One of these possible forms gives us a reference frame in Figure 2. The direction cosines denoted by θ_x and θ_y in the figure are specified to define the antenna field of view. to the large antenna field in JRO and obtain the reference frame as in Figure 2.

A single $\hat{x}$-polarized antenna will transmit $\hat{p}_x = \frac{\hat{k}\times\hat{k}\times\hat{x}}{|\hat{k}\times\hat{k}\times\hat{x}|}$ polarized radiowaves in $\hat{k}$ direction . In reception, two orthogo-

nal linearly polarized antennas are used to collect the backscattered signal. The magnetic aspect angle is the complement of the angle θ between the magnetic field vector and propagation direction. In small magnetic aspect angle approximation, θ is around $90°$.

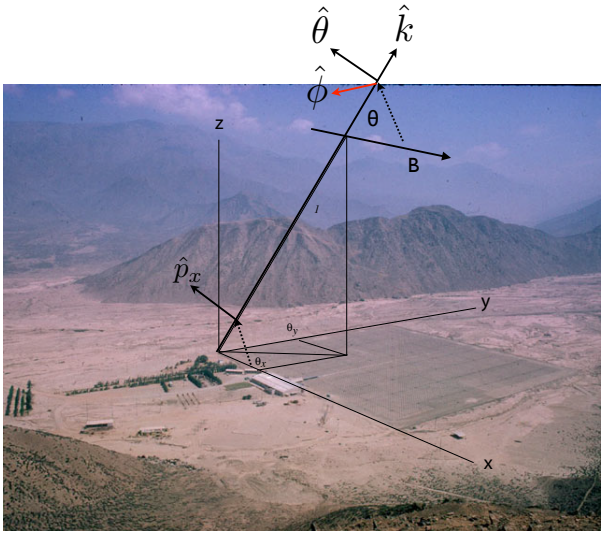

Figure 2. Representation of direction cosines and the direction of the beam over antenna field.

In a magnetized plasma, there are two possible and orthogonal modes of electromagnetic wave propagation. These modes are known as *ordinary (*O*)* and *extra*ordinary (X). Electric field component of a radiowave propagating in a magnetized plasma can be expressed as weighted superposition of these modes of propagation. Hence, an electric field radiating from the origin along a distance r in a cold plasma can be written as [9]

$$\vec{E}^t = A_O \left(\hat{\theta} - j\hat{\phi}\frac{F_O}{Y_L}\right) e^{-jk_o n_O r} + A_X \left(\hat{\theta} - j\hat{\phi}\frac{F_X}{Y_L}\right) e^{-jk_o n_X r}, \tag{1}$$

where A_O anand d A_X are the amplitudes of the elliptically polarized O- and X-mode propagating waves. Polarization relations $\frac{F_O}{Y_L}$ and $\frac{F_X}{Y_L}$ in (1) determine the type of polarization and yield the *Appleton-Hartree* refractive indices [9]

$$n^2_{O/X} = 1 - \frac{X}{1 - F_{O/X}},$$

where

$$F_{O/X} = \frac{Y_T^2 \pm \sqrt{Y_T^4 + 4(1-X)^2 Y_L^2}}{2(1-X)},$$

and

$$X \equiv \frac{\omega_p^2}{\omega^2}, \quad Y_L \equiv \frac{\Omega_e}{\omega}\cos\theta, \text{ and } \quad Y_T \equiv \frac{\Omega_e}{\omega}\sin\theta,$$

with

$$\omega_p \equiv \sqrt{\frac{N_e q_e^2}{\epsilon_o m_e}}, \text{ and } \Omega_e \equiv \frac{eB_o}{m_e},$$

ω_p and Ω_e are the plasma frequency and gyrofrequency. In the equations above, ω is the operating frequency, N_e, the electron density, q_e the electron charge, m_e the mass of an electron charge, ϵ_o the electrical permittivity for free-space and B_o is the magnitude of the local magnetic field vector.

Considering a radiowave propagating in an arbitray direction in a magnetized inhomogeneous ionosphere, we will divide the ionosphere into slabs of 5 km-width perpendicular to the propagation direction to model the electric field component of the incoherent scattered radar signal. In Figure 3, Δr is the slab width and slabs are numbered from 1 to 200 to cover a distance of 1000 km.

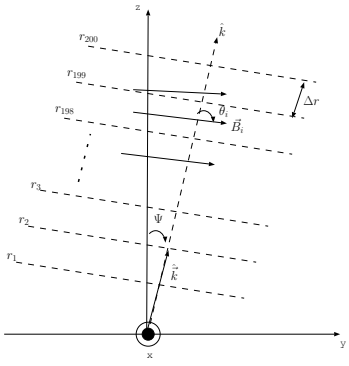

Figure 3. Geometry of wave propagation in an inhomogeneous magnetized ionosphere [9].

To analyze the electric field components of the incoherent scattered signal propagating through the slabs, we will use a propagator matrix, $\bar{T}$ that will map the electric field components in one slab to the next slab. Thus, the total electric field in (1) can be recast in a matrix form as

$$\begin{bmatrix} E_\theta \\ E_\phi \end{bmatrix} \propto \bar{T} \cdot \begin{bmatrix} E_{\theta o} \\ E_{\phi o} \end{bmatrix}, \tag{2}$$

where $E_{\theta,o}$ and $E_{\phi,o}$ are the field components at the origin. Note that when $r = 0$, $\vec{E}^t|_{r=0} \equiv \vec{E}^t_o$.

By defining $\bar{n} = (n_O + n_X)/2$ and $\Delta n = (n_O - n_X)/2$, the propagator matrix, $\bar{T}$ is given by [9]

$$\bar{T} \equiv \frac{e^{-jk_o\bar{n}r}}{1+a^2}\begin{bmatrix} e^{-jk_o\Delta nr} + a^2 e^{jk_o\Delta nr} & 2a\sin(k_o\Delta nr) \\ -2a\sin(k_o\Delta nr) & a^2 e^{-jk_o\Delta nr} + e^{jk_o\Delta nr} \end{bmatrix},$$

where a is the axial ratio defined as the ratio of the transverse components of the electric field, i.e. $a \equiv \frac{E_\theta}{E_\phi}$.

The propagator matrices will be used for the propagation of the radar signals through atmospheric slabs. The transmitted and reflected radiowaves will excite both ordinary and extraordinary propagation modes in the plasma. Hence, the values of matrix elements as well as $\vec{E}_\theta$ and $\vec{E}_\phi$ will evolve from slab to slab. The same propagator matrices will be used to propagate the the fields back from a distance r to the origin [7]. The forward and backward propagation model composed of the propagator matrices particular to each slab can be written

$$\begin{bmatrix} E_\theta \\ E_\phi \end{bmatrix} = T_1 T_2 T_3 \ldots T_r T_r \ldots T_3 T_2 T_1 \begin{bmatrix} E_{\theta o} \\ E_{\phi o} \end{bmatrix}.$$

From (2), we can also recast the radiated electric field phasor propagating from one slab to the next as [7]

$$\vec{E}_i = e^{-jk_o\bar{n}_i\Delta r}\left[e^{-jk_o\Delta n_i\Delta r} p_O p_O^H + e^{jk_o\Delta n_i\Delta r} p_X p_X^H\right]\vec{E}_{i-1},$$

and

where $\vec{E}_i = \vec{E}_{\theta_i}\hat{\theta} + \vec{E}_{\phi_i}\hat{\phi}$ is the superposition of the propagation modes at $i-th$ slab. Also, p_O and p_X are polarization vectors of the O- and X-mode waves given by

$$p_O = \frac{\hat{\theta}_i - ja\hat{\phi}_i}{\sqrt{1+a_i^2}} \quad \text{and} \quad p_X = \frac{-ja\hat{\theta}_i + \hat{\phi}_i}{\sqrt{1+a_i^2}},$$

whose conjugate transposes are denoted as p_O^H and p_X^H.

At the ground level, the incoherent scattered signal will be received by both antennas oriented perpendicular to one another. Thus, we multiply the down-coming field with co- and cross-polarized single dipole antennas and find the co- and cross-polarized complex open circuit voltages as

$$\upsilon_x \propto \hat{p}_x.(E_\theta\hat{\theta} + E_\phi\hat{\phi}),$$
$$\upsilon_y \propto \hat{p}_y.(E_\theta\hat{\theta} + E_\phi\hat{\phi}),$$

respectively. Utilizing these co- and cross-polarized voltages, we can build a covariance matrix as

$$\text{CovMat} = \begin{bmatrix} |\upsilon_x|^2 & \upsilon_x^*\upsilon_y \\ \upsilon_x\upsilon_y^* & |\upsilon_y|^2 \end{bmatrix}_i$$

where i denotes the number of the slab.

III. Model Results and Discussion

We will present the co- and cross-polarized voltages of the received signals to demostrate the magneto-ionic effects. In the following figures, the co- and cross-polarized received signals are plotted in blue and red , respectively. The electron density profile used in our model is shown in Figure 4 [7]. The hypothetical elctron density model with one hump is not too far away from the daytime realistic cases.

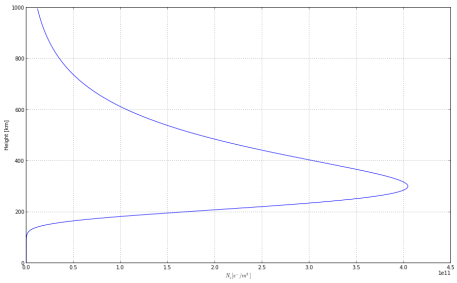

Figure 4. Electron density vs. range.

Radar targets seen by the Jicamarca beam are referenced in terms of their direction cosines in the range$\theta_{x,y}$ in $[-0.147, 0.147]$. In the model this range of direction cosines are discretized over a 13×13 grid with 0.0245 grid spacings. Figure 5 displays the co- and cross-variance profiles computed at each of these grid points.

In Figure 5 magnetic aspect angle varies diagonally from lower right to upper left and we note that variance profiles are relatively invariant in the orthogonal direction going from lower left to upper right of Figure 5. Hence, our model can be based on a simpler (and computationally faster) gridding of the radar field of view shown in Figure 6 having fine sampling in the north-south direction (vertical in the figure) but coarse sampling in the east west direction (horizontal in the figure) and having a zig-zag topology as shown. Covariance profiles computed at the vertices of the displayed zig-zag grid can be used to compute off-grid profiles using simple interpolations of the profiles computed at the vertices of the triangles enclosing the off-grid points.

Altitude variations of the covariances shown in Figure 6 are consistent with the fact that electron density (N_e) is peaked approximately 300 km altitudes and is negligible below 100 km in compliance with the N_e profile shown in Figure 4. Again densities and magnetoionic effects diminish as 1000 km altitude is approached.

Magneto-ionic effects are results of magnetoplasma. In our model, magneto-ionic effects have been observed in two different angular regimes of ionosphere. When the magnetic field is *perpendicular* to the propagation direction of the beam, a linearly polarized wave can become elliptical due to the different phase velocities of the X- and O-modes. This elliptization effect is known as *Cotton-Mouton effect*. When the beam is pointed off perpendicular to Earth's magnetic field, the beam experiences *Faraday effect* (or *Faraday Rotation*). In this case, the characteristic modes become circularly polarized.

These magneto-ionic effects are observed in Figure 6. When the beam points *off perpendicular* to Earth's magnetic field, we observe wiggles in Faraday-regime. However, in the Cotton-Mouton regime we see almost no wiggle. These two magneto-ionic effects valid along the heights where magnetoplasma takes place are the main effects on the incoherent scattered radar signal during its travel through ionosphere.

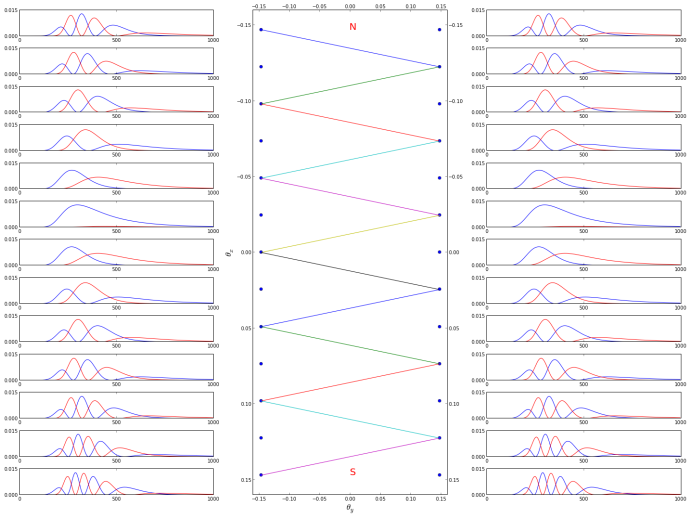

Figure 6. Covariance values in a two-dimensional reduced grid.

IV. Conclusions and Future Work

We have presented in this report how the polarization of incoherent scattered radar signals traveling in a magnetized ionosphere will vary as a function of scattering altitudes. We were able to model the Faraday and Cotton-Mouton effects on incoherent radar signals traveling at different magnetic aspect angles. In the simulations we also showed the range limits of ionosphere and the relationship between the strength of magnetoionic effects and N_e. In future work the model presented here will be a component of a larger data inversion

tool to be used for fitting the measured ISR spectra at small magnetic aspect angles with theoretical ISR spectra with ionospheric input parameters of interest.

REFERENCES

[1] Dougherty, J. P., and D. T. Farley (1960), A theory of incoherent scattering of radio waves by a plasma, Proceedings of the Royal Society of London. Series A, Mathematical and Physical Sciences, 259 (1296). <return>

[2] Farley, D. T., J. P. Dougherty, and D. W. Barron (1961), A theory of incoherent scattering of radio waves by a plasma ii. Scattering in a magnetic field, Proceedings of the Royal Society of London. Series A, Mathematical and Physical Sciences, 263 (1313), 238–258.

[3] Fejer, J. A. (1961), Scattering of radio waves by an ionized gas in thermal equilibrium in the presence of a uniform magnetic field, Canadian Journal of Physics, 39, 716–740.

[4] Farley, D. T. (1964), The effect of Coulomb collisions on incoherent scattering of radio waves by a plasma, Journal of Geophysical Research, 69 (1), 197–200, doi:10.1029/ JZ069i001p00197.

[5] Woodman, R. F. (1967), Incoherent scattering of electromagnetic waves by a plasma, Ph.D. dissertation, Harvard University, Cambridge, Massachusetts, 1967.

[6] Kudeki, E., Bhattacharyya,S., and R. F. Woodman (1999), A new aproach in incoherent scatter F region $\vec{E} \times \vec{B}$ drift measurement at Jicamarca, Journal of Geophysical Research, 104 (A12), 28145–28162.Milla,M., Study of Coulomb Collisions and Magneto-ionic Propagation Effects on Incoherent Scatter Radar Measurements at Jicamarca, PhD Thesis, 2010.

[7] Kudeki, E.; Milla, M.A.; , "Incoherent Scatter Spectral Theories—Part I: A General Framework and Results for Small Magnetic Aspect Angles," Geoscience and Remote Sensing, IEEE Transactions on , vol.49, no.1, pp.315-328, Jan. 2011

[8] Milla, M.A.; Kudeki, E.; , "Incoherent Scatter Spectral Theories—Part II: Modeling the Spectrum for Modes Propagating Perpendicular to B ," Geoscience and Remote Sensing, IEEE Transactions on , vol.49, no.1, pp.329-345, Jan. 2011

[9] Erhan Kudeki and Marco Milla (2012). Incoherent Scatter Radar - Spectral Signal Model and Ionospheric Applications, Doppler Radar Observations - Weather Radar, Wind Profiler, Ionospheric Radar, and Other Advanced Applications, Dr. Joan Bech (Ed.), ISBN: 978-953-51-0496-4, InTech, DOI: 10.5772/39010.

Figure 5. Representation of antenna field by a sampled grid.

B. LEVENT GEZER

Coordinated Science Lab. Room 312,
University of Illinois at Urbana-Champaign
(217) 979 67 68

OBJECTIVE

To present my knowledge and experience in remote sensing and electromagnetics before the committee.

EDUCATION

PhD	Electrical Engineering University of Illinois	Remote Sensing at Urbana-Champaign	*Sep'11- con'ing*
MSSE	Systems Engineering Naval Postgraduate School	Electronic Warfare Systems Monterey, CA	*Sep `04 - Sep `06* *GPA* 3.82 (4.0 Scale)
BSEE	Electrical Engineering Turkish Naval Academy	Communications Istanbul, Turkey	*Aug `96 - Aug`00* *GPA* 3.31 (4.0 Scale)

SKILLS

●Python ● MATLAB ●LabVIEW

Design Experience :

- Designed and developed a phased array tracking antenna system.
- Determined the components in the system and characterized them with a network analyzer.
- Developed a computer model in MATLAB and LabVIEW to analyze the RF pattern of the system.
- Ran tests on the system in an anechoic chamber.

PROFESSIONAL EXPERIENCE

Unv.of Illinois at Urbana-Champaign Champaign, IL Jan 2013 – cont`ing

- Working as a Teaching Assistant for ECE 350 (Fields and Waves I) given by Prof. E.KUDEKI
- Holding Office hours twice a week and review sessions before the midterms
- Preparing homework solutions

Jicamarca Radio Observatory Peru Internship May-July 2012

- Converted the codes related to Magnetoionic Propagation from MATLAB to Python
- Joined journal discusssion groups and seminars.

Unv.of Illinois at Urbana-Champaign Champaign, IL Sep 2011 – Jan 2013

- Worked as a Research Assistant under the supervision of Prof. E.KUDEKI
- Took courses ECE468 (Optical Remote Sensing), ECE520 (EM Waves and Radiating Systems), ECE531 (Theory of Guided Waves) and ECE569 (Inverse Problems in Optics).

Turkish Navy Turkey Systems Engineer *Sep `06- present*

- Managed the technical department of the Integrated Maritime Surveillance System (IMSS), a radar and communications network, with a $ 500 million budget.
- Participated in acceptance tests of radar and software of comms. systems as a test engineer.
- Supervised the installation of radars and Electronic Support Measurements (ESM) systems.

Turkish Navy Turkey Electronic Maintenance Officer *Nov `00- Aug`04*

- Supervised 15 technicians and 16 operators on a battleship.
- Responsible for maintenance and reparation of the radars, EW and communication systems.

PUBLICATIONS

Levent GEZER, Robert BROADSTON, David Jenn & Gert BERGSTALLER, *Digital Tracking Array Using Off-The-Shelf Hardware,* IEEE Antennas&Propagation, 2008 Vol. 50 Issue 1.

B.L.Gezer, D.Kuntalp, M.Kuntalp, *Clustering of Arrhythmic ECG Beats Using Morphological Properties and Windowed Raw ECG Data*, April 20-22 2011, 19th IEEE Conference on Signal Processing and Communications Applications.